SCIENTIFIC REPORTS

OPEN

SUBJECT AREAS:
TRANSMISSION ELECTRON MICROSCOPY
STRUCTURAL PROPERTIES

Received
25 November 2013

Accepted
26 February 2014

Published
18 March 2014

Correspondence and requests for materials should be addressed to J.W. (wangj6@lanl.gov); S.K.G. (gongsk@buaa.edu.cn) or S.X.M. (smao@engr.pitt.edu)

Atomistic observation of a crack tip approaching coherent twin boundaries

L. Liu[1], J. Wang[2], S. K. Gong[1] & S. X. Mao[3]

[1]School of Materials Science and Engineering, Beihang University, Beijing 100191, People's Republic of China, [2]MST-8, MS G755, Los Alamos National Laboratory, Los Alamos, NM 87545, USA, [3]Department of Mechanical Engineering and Materials Science, University of Pittsburgh, Pittsburgh, Pennsylvania 15261, USA.

Coherent twin boundaries (CTBs) in nano-twinned materials could improve crack resistance. However, the role of the CTBs during crack penetration has never been explored at atomic scale. Our in situ observation on nano-twinned Ag under a high resolution transmission electron microscope (HRTEM) reveals the dynamic processes of a crack penetration across the CTBs, which involve alternated crack tip blunting, crack deflection, twinning/detwinning and slip transmission across the CTBs. The alternated blunting processes are related to the emission of different types of dislocations at the crack tip and vary with the distance of the crack tip from the CTBs.

Σ3 {111} CTBs are mechanically and thermally stabilized interfaces in face-centered cubic (FCC) metals for their high coherency and low excessive energy[1]. During the past decade, materials containing high-density CTBs have been examined to have high strength and hardness without overly compromising ductility, fracture toughness, thermal stability and electrical conductivity[2–8]. The strengthening effect is ascribed to the discontinuity of slip systems across CTBs and the dislocation reaction occurring at CTBs[9–13]. Recently, the softening effect in association with the CTB migration has been observed in nano-twined materials when the twin thickness decreases below a few nanometers[4,14–20].

In contrast to the numerous studies regarding the strengthening and softening effects of the CTBs in materials, the role of the CTBs in toughening materials is rarely studied, particularly at atomistic scale. Molecular dynamics (MD) simulations have been used to investigate the crack-CTB interaction in nano-grained nickel with nanoscale twins[21,22]. It was found that massive partial dislocations are activated and glide on the CTBs when the crack tip is drawing near, enhancing the fracture resistance of nano-grained copper[22]. In addition, the daughter cracks along the neighboring CTBs also provide efficient shielding to the mother crack[22]. Another MD simulation suggested that the dislocations accumulated along the CTBs ahead of the crack tip provide enough strain hardening to result in more uniform plastic deformation, consequently toughening the material[20,23]. In situ transmission electron microscope (TEM) offers a powerful tool for the real time observation on deformation mechanisms. By this mean, it was observed that the crack propagation path was deflected when the crack penetrated the CTBs and the dislocations that locate at the CTBs were functional to arrest the crack tip, rendering crack resistance to the metallic thin film[24,25]. However, the experimental evidence at atomistic scale is still lacking. In this letter, we report the HRTEM observation of the crack penetrating the CTBs at atomistic scale. In accompany with our MD simulation, a better understanding is provided to the role of the CTBs in the deformation and fracture mechanisms.

Results

A series of HRTEM images in Fig. 1 reveal the dynamic processes of the crack penetrating the CTBs, which involve plastic deformation modes, crack path deflection and crack tip blunting.

First, diverse plastic deformation phenomena are observed. Dislocations emit from the crack tip and the crack surfaces, and glide on {111} planes that are parallel to the CTBs and towards the CTBs like P3 plane (denoted in Fig. 1 (b)). Most of these dislocations are Shockley partial dislocations, followed by stacking fault (SF), in response to the low stacking fault energy (SFE) of silver[26]. These dislocations are hindered by the upper CTB (two CTBs in the observed region) and remain in the extended character–partial dislocations linked to the CTB by SF. This is in coincidence with the previous reports[3,20], giving rise to the desirable strain hardening in the CTB-strengthened materials. Driven by successive loading pulses, some of these dislocations can transmit across the CTB, glide through the twin and arrive at the lower CTB as indicated in Fig. 1 (a). The dislocation transmission leads to the

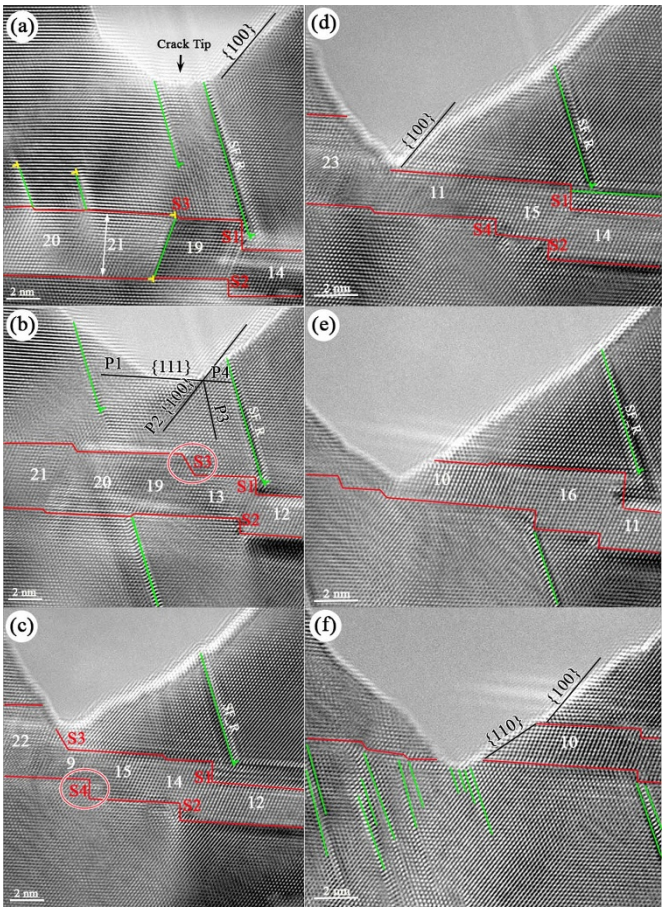

Figure 1 | (a) to (c) in situ HRTEM images during the crack propagation in the matrix. (d) to (f) in situ HRTEM images during the penetration of the crack across the CTBs. The beam direction is parallel to <110>. The CTBs are outlined in red lines and the corresponding twin thickness is labeled in the unit of layers. A stacking fault marked as SF_R is chosen as the reference. The crack surface changes from {100} to {110} after the crack penetration across the CTBs. P1, P2, P3 and P4 in (b) indicate slip planes.

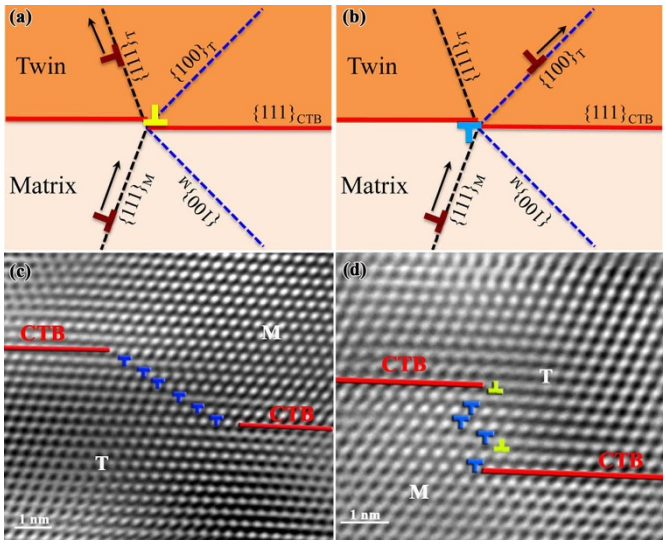

Figure 2 | **A full mixed-type dislocation transfers across a CTB through two possible reactions.** (a) from $\{111\}_M$ to $\{111\}_T$, leaving a residual dislocation at the CTB which is an edge-type Shockley partial dislocation (corresponding to $1/2<110>\{111\}_M \rightarrow 1/2<110>\{111\}_T + 1/6<112>\{111\}_{CTB}$ (edge-type)) and (b) from $\{111\}_M$ to $\{100\}_T$, leaving a residual dislocation at the CTB which is a mixed-type Shockley partial dislocation (corresponding to $1/2[110]\{111\}_M \rightarrow 1/2<110>\{100\}_T + 1/6<112>\{111\}_{CTB}$ (mixed-type)). Arrows indicate the glide directions of the dislocations. (c) HRTEM image showing the dislocation structures of the ledge S3 in Fig. 1 (b) containing all same-sign partials. (d) The HRTEM image of the sharp ledge S4 in Fig. 1 (c) containing partials with the net zero Burgers vectors. The blue and yellow "T"s are for the mixed-type and edge-type partial dislocations respectively, while the brown "T"s are for full dislocations.

CTB ledges, marked as S1–S4 in Fig. 1, which are composed of multiple partial dislocations. The formation of these partial dislocations has been demonstrated by MD simulations[11,20,27,28] and observed experimentally with TEM[29,30]. The formation mechanisms are described as following: a full dislocation transmits across a CTB through two possible dislocation reactions with respect to the stress state, either $1/2<110>\{111\}_M \rightarrow 1/2<110>\{111\}_T + 1/6<112>\{111\}_{CTB}$ (edge-type)[27] or $1/2<110>\{111\}_M \rightarrow 1/2<110>\{100\}_T + 1/6<112>\{111\}_{CTB}$ (mixed-type)[11], as illustrated in Fig. 2 (a) and (b) respectively. Each reaction creates one partial dislocation left on the CTB. Correspondingly, continuous reactions of different types will increase the height of the ledges. Fig. 2 (c) and (d) show the atomic structures of the dislocation ledges S3 and S4 indicated in Fig. 1 (b) and (c), where partial dislocations on every {111} plane can be distinguished. The dislocation ledge S4 in Fig. 2 (d) is sharp and composed of two kinds of partial dislocations, which involves both the reactions that are illustrated in Fig. 2 (a) and (b). The ledges S1 and S2 also contains different partial dislocations. These structures are similar to Σ3 {112} incoherent twin boundaries frequently observed in fcc metals[14,18,31], although the stacking sequence is slightly different. In contrast, the dislocation ledge S3 in Fig. 2 (c) is composed of the same partial dislocations in response to the same dislocation reaction. The dislocation structures of S1, S2 and S4 are energetically more favorable than S3 because the Burgers vectors of different partial dislocations cancel each other and result in much lower net strain. The motion of the ledges is affirmed in Fig. 1 (b) to (d), which accounts for the migration of the CTB and the reduction of the twin thickness (detwinning)[17,25,31]. As seen in Fig. 1, the mobility of the ledge S3 is better than S1, S2 and S4, which is ascribed to the identical twinning dislocations in the ledge S3. The twinning/detwinning is also induced directly by the emission of partial dislocations at the crack tip and their gliding on the CTB (Fig. 1 (c) to (e)). In addition, the ledge S1 is restrained and does not move because of the SF (denoted as SF_R in Fig. 1)[15]. It is noteworthy that the dislocation reactions described above are usually intermediated by partial dislocations due to the low SFE of Ag. As seen in Fig. 1 (a), an SF is confined within the twin band with stair-rod dislocations at both ends. The upper stair-rod dislocation is generated by the reaction– $1/6<211>\{111\}_M + 1/6<121>\{111\}_M \rightarrow 1/6<211>\{111\}_T + 1/6<121>\{111\}_T + 1/6<112>\{111\}_{CTB} \rightarrow 1/6<211>\{111\}_T +$ (stair-rod dislocation)[27]. The lower stair-rod dislocation is formed when the product partial $1/6<211>\{111\}_T$ arrives at the lower CTB. However, the stair-rod dislocations can dissociate into mobile partial dislocations again. In Fig. 1 (b), the confined SF has disappeared and the ledge S3 is formed by the repetition of the same dislocation reactions.

The deflection of the crack propagation path is also observed in Fig. 1. By the reference of the stacking fault, SF_R, the crack tip moves towards the left in Fig. 1 (a) to (b) and the right crack surface is close to {100} as marked in Fig. 1 (a). Based on the beam direction along <110>, the propagation direction on the {100} surface is determined as <110>, which implies the slips on two planes are preferred: {111} plane on the left of the crack tip (parallel to the CTB as denoted P1 in Fig. 1 (b)) and {100} plane (parallel to the crack surface as denoted P2). This can be ascribed to the presence of the stacking fault, SF_R, which obstructs the emission and gliding of dislocations towards the

right of the crack tip. However, the crack tip moves perpendicularly to the CTB during penetrating the twin (Fig. 1 (d) to (e)). Considering the unchanged shape of the lower CTB and the completely detwinned left part, the favored slip mode in this period is the dislocations on P1 and the rupture of atom bonds takes place at the crack tip to accomplish the brittle-like crack propagation. The slips on P4 are probably still hindered by SF_R. As a consequence, the crack surface changes from {100} in the matrix to {110} in the twin, and the propagation direction changes from <110> in the matrix to <100> in the twin. After the transmission, slips operate on {111} planes non-parallel to the CTB, resulting in the propagation towards right and the SFs in Fig. 1 (f). Such a deflection of the crack path implies that the crack propagation direction is influenced by both the CTBs and local microstructures (like SF_R).

The most interesting phenomenon in Fig. 1 is the alternated blunting of the crack tip. The crack tip is blunted in the matrix when it is far away from the CTBs as in Fig. 1 (a) and (b), becomes sharp when the crack approaches the upper CTB in Fig. 1 (c) and (d), much sharper in the twin as observed in Fig. 1 (e), and is blunted again in Fig. 1 (f) after it penetrates the lower CTB. According to the criterion for dislocation nucleation versus cleavage by J. R. Rice[32], silver is usually incapable of brittle-like cracking, so the observation of the sharp crack tip is surprising. (Detailed calculation and analysis related to the fracture resistance can be found in Supplementary Information.) Corresponding to different deformation modes discussed in the above section, we believe that the variation of the crack morphology is ascribed to the different dislocation emission activity at the crack tip. When the crack is far from or across the CTBs, it is obvious that the crack tip is blunted in association with the slips on multiple slip systems P1 to P4 in Fig. 1 (a), (b) and (f). When the crack is close to the CTBs, the slip systems are severely suppressed as explored in Fig. 1 (c) to (d), due to the shielding of the dislocations accumulated at the CTBs, leading to the sharpening of the crack tip. The high stress state at the CTBs can be inferred from the distorted lattice ahead of the crack in Fig. 1 (e). However, if the slip systems parallel to the CTBs are activated when the crack tip is very close, the crack can still be blunted at some level. As in Fig. 1 (c), since the twin is curved by the ledges, the crack tip is adjacent to part of the CTB in the assistance of the ledge S3. So the emission of partial dislocations to the left side along the CTB is favored, owing to the negligible energy change of the CTB migration[17]. In contrast, when neither of the CTBs is adjacent, as in Fig. 1 (e), the emission of the partial dislocation along the CTB is difficult since otherwise it will introduce a new SF and increase the total energy significantly, so the crack tip is much sharper than that in Fig. 1 (c).

In order to understand the above plastic and fracture processes, we conducted MD simulation for nano-twinned silver as shown in Fig. 3 (the details can be seen in Supplementary Information). Both the slip transmission and slips along the CTBs agree with the plastic deformation modes in Fig. 1. An extended full dislocation emits from the crack tip in Fig. 3 (a), glides on the {111} plane non-parallel to the CTBs (corresponding to P3 in Fig. 1) and transfers to the {111} plane in the twin, leaving a dislocation ledge on the CTB. Simultaneously, partial dislocations glide on the CTB adjacent to the crack tip (P4) and result in the CTB migration. The crack tip isn't blunted efficiently because of another CTB in front of the crack tip with short distance in Fig. 3 (a) and (b). However, when the crack tip arrives at the CTB, the slips along the CTB (both P1 and P4) are further enhanced as seen in Fig. 3 (c) and the crack is blunted more intensely. Correspondingly, the blunted crack tip slows down the crack propagation as observed in MD simulation (the movie in Supplementary Video). Then, the two twins on the right part are merged in associated with the CTB migration, so the original P4 slip system is deactivated and the crack tip is sharp again during the subsequent propagation in Fig. 3 (d). Compared to the experimental results in Fig. 1, the blunting of the crack in Fig. 3 is generally less pronounced

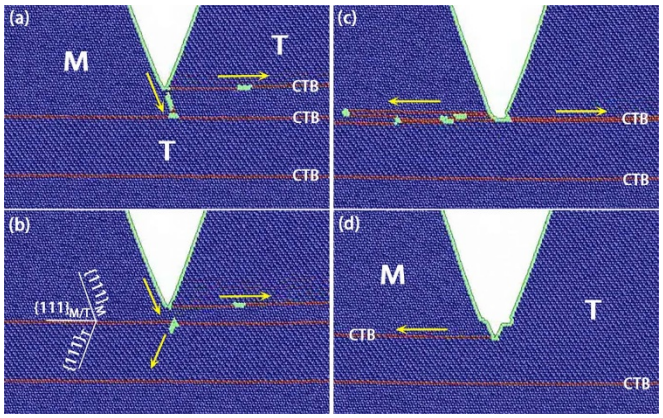

Figure 3 | MD simulation of cracking a nanotwinned Ag. Shockley partial dislocations emit at the crack tip and glide towards the right in (a, b) before the crack penetrates the CTB, and towards the left in (c, d) after the penetration across the CTB. Disregistry analysis indicates these partials are 30° mixed partial dislocations. A full dislocation emits at crack tip in (a), is blocked at the CTB and transfer into the twin in (b). More partials emit and the crack tip is blunted in (c). The crack tip becomes sharp again when close to the next CTB in (d). The yellow arrows indicate the gliding directions. "M" and "T" mean matrix and twin respectively. The CTBs and atom planes are denoted in white characters. Atoms are colored according to the Common-Neighbor-Analysis. The Blue represents fcc, the red represents hcp, and the green represents the disordered, i.e. surfaces and dislocation cores.

because of the high stress and the low temperature in the MD simulation. However, it is in agreement that crack tip can be blunted more efficiently if adjacent to the CTBs.

Discussion

It can be inferred from the experiment and the MD simulation that the fracture behavior is strongly influence by the distance between the crack tip and the CTBs. If the crack is away from the upfront CTBs, it propagates in a ductile manner as expected. If close to the CTBs, the crack appears more brittle-like, compromising the crack resistance. Limited crack blunting is retained when the crack is adjacent to the CTBs due to the slips along the CTBs, but apparently the slips non-parallel to the CTBs play a more important role in the alternated crack blunting process. As a consequence, in nanotwinned structures, different twin thickness imparts not only different strength but also different fracture resistance to the materials[6,7]. Therefore, specific combined mechanical properties can be tuned to suit certain service circumstance by tailoring twin thickness.

In conclusion, we have studied the atomic-level mechanisms of the crack propagation across the CTBs by in situ stretching Ag film in HRTEM. Different deformation modes, including dislocation transmission across the CTBs, CTB migration and twinning/detwinning, have been found. The results provide insights into the alternated crack blunting mechanisms when crack approaching CTBs. The closer the crack is to the CTBs, the sharper the crack tip is, because of the more suppressed slip systems. The slips on the CTBs can facilitate blunting if the crack is adjacent to the CTBs but with relatively lower efficiency. The crack propagation path is deflected from <110> in the matrix to <100> in the twin by the influence of the CTBs and the local microstructures. The results suggest that an optimized twin thickness exists with regards to coordinating the strength and fracture resistance of nano-twinned materials.

Methods

High purity 99.99% polycrystalline Ag film with the thickness of 100 μm was used in this experiment. The film was cut into 11.5 × 2.5 mm rectangles to fit the Gatan single tilt straining holder. The middle of the specimens was thinned by double-jet

electropolishing in the solution of 10% perchloric acid, 10% glycerol and 80% methanol at 213 K in a TenuPol-5 eletropolisher. The TEM observation was conducted at room temperature using a JEM2100F field-emission microscope with point-to-point resolution of 0.23 nm. The configuration in Fig. 1 is formed during in situ stretching the Ag film in TEM. The notch is the crack, which was generated at the edge of the thinned area and propagated into this grain. The twin lamella was produced when the crack tip was approaching, owing to the activated partial dislocation slip in this grain under applied loadings.

1. Wang, J., Li, N. & Misra, A. Structure and stability of Σ3 grain boundaries in face centered cubic metals. *Philos. Mag.* **93**, 315–327 (2012).
2. Lu, L., Shen, Y., Chen, X., Qian, L. & Lu, K. Ultrahigh Strength and High Electrical Conductivity in Copper. *Science* **304**, 422–426 (2004).
3. Lu, L., Chen, X., Huang, X. & Lu, K. Revealing the Maximum Strength in Nanotwinned Copper. *Science* **323**, 607–610 (2009).
4. Li, X., Wei, Y., Lu, L., Lu, K. & Gao, H. Dislocation nucleation governed softening and maximum strength in nano-twinned metals. *Nature* **464**, 877–880 (2010).
5. Anderoglu, O., Misra, A., Wang, H. & Zhang, X. Thermal stability of sputtered Cu films with nanoscale growth twins. *J. Appl. Phys.* **103**, 094322 (2008).
6. Qin, E. W., Lu, L., Tao, N. R. & Lu, K. Enhanced fracture toughness of bulk nanocrystalline Cu with embedded nanoscale twins. *Scr. Mater.* **60**, 539–542 (2009).
7. Singh, A., Tang, L., Dao, M., Lu, L. & Suresh, S. Fracture toughness and fatigue crack growth characteristics of nanotwinned copper. *Acta Mater.* **59**, 2437–2446 (2011).
8. Wang, J., Sansoz, F., Huang, J., Liu, Y., Sun, S., Zhang, Z. & Mao, S. X. Near-ideal theoretical strength in gold nanowires containing angstrom scale twins. *Nat. Commun.* **4**, 1742 (2013).
9. Deng, C. & Sansoz, F. Repulsive force of twin boundary on curved dislocations and its role on the yielding of twinned nanowires. *Scr. Mater.* **63**, 50–53 (2010).
10. Lee, J. H., Holland, T. B., Mukherjee, A. K., Zhang, X. & Wang, H. Direct observation of Lomer-Cottrell Locks during strain hardening in nanocrystalline nickel by in situ TEM. *Sci. Rep.* **3**, 1061 (2013).
11. Wang, J. & Huang, H. Novel deformation mechanism of twinned nanowires. *Appl. Phys. Lett.* **88**, 203112 (2006).
12. Deng, C. & Sansoz, F. Near-Ideal Strength in Gold Nanowires Achieved through Microstructural Design. *ACS Nano* **3**, 3001–3008 (2009).
13. Deng, C. & Sansoz, F. Enabling Ultrahigh Plastic Flow and Work Hardening in Twinned Gold Nanowires. *Nano Lett.* **9**, 1517–1522 (2009).
14. Wang, J., Misra, A. & Hirth, J. P. Shear response of Σ3{112} twin boundaries in face-centered-cubic metals. *Phys. Rev. B* **83**, 064106 (2011).
15. Li, N., Wang, J., Zhang, X. & Misra, A. In-situ TEM study of dislocation-twin boundaries interaction in nanotwinned Cu films. *JOM* **63**, 62–66 (2011).
16. Li, N., Wang, J., Misra, A., Zhang, X., Huang, J. Y. & Hirth, J. P. Twinning dislocation multiplication at a coherent twin boundary. *Acta Mater.* **59**, 5989–5996 (2011).
17. Wang, J., Li, N., Anderoglu, O., Zhang, X., Misra, A., Huang, J. Y. & Hirth, J. P. Detwinning mechanisms for growth twins in face-centered cubic metals. *Acta Mater.* **58**, 2262–2270 (2010).
18. Wang, J., Anderoglu, O., Hirth, J. P., Misra, A. & Zhang, X. Dislocation structures of Σ3 {112} twin boundaries in face centered cubic metals. *Appl. Phys. Lett.* **95**, 021908 (2009).
19. Wang, J., Huang, H., Kesapragada, S. V. & Gall, D. Growth of Y-Shaped Nanorods through Physical Vapor Deposition. *Nano Lett.* **5**, 2505–2508 (2005).
20. Zhu, T. & Gao, H. Plastic deformation mechanism in nanotwinned metals: An insight from molecular dynamics and mechanistic modeling. *Scr. Mater.* **66**, 843–848 (2012).
21. Zhou, H. F. & Qu, S. X. The effect of nanoscale twin boundaries on fracture toughness in nanocrystalline Ni. *Nanotechnology* **21**, 35706 (2010).
22. Zhou, H. F., Qu, S. X. & Yang, W. Toughening by nano-scaled twin boundaries in nanocrystals. *Model. Simul. Mater. Sci. Eng.* **18**, 65002 (2010).
23. Zhu, L., Ruan, H., Li, X., Dao, M., Gao, H. & Lu, J. Modeling grain size dependent optimal twin spacing for achieving ultimate high strength and related high ductility in nanotwinned metals. *Acta Mater.* **59**, 5544–5557 (2011).
24. Kim, S. W., Li, X., Gao, H. & Kumar, S. In situ observations of crack arrest and bridging by nanoscale twins in copper thin films. *Acta Mater.* **60**, 2959–2972 (2012).
25. Shan, Z. W., Lu, L., Minor, A. M., Stach, E. A. & Mao, S. X. The effect of twin plane spacing on the deformation of copper containing a high density of growth twins. *JOM* **60**, 71–74 (2008).
26. Hirth, J. P. & Lothe, J. *Theory of Dislocations* (Krieger, Melbourne, FL, 1992).
27. Jin, Z. H., Gumbsch, P., Albe, K., Ma, E., Lu, K., Gleiter, H. & Hahn, H. Interactions between non-screw lattice dislocations and coherent twin boundaries in face-centered cubic metals. *Acta Mater.* **56**, 1126–1135 (2008).
28. Yamakov, V., Wolf, D., Phillpot, S. R. & Gleiter, H. Dislocation–dislocation and dislocation–twin reactions in nanocrystalline Al by molecular dynamics simulation. *Acta Mater.* **51**, 4135–4147 (2003).
29. Sennour, M., Lartigue-Korinek, S., Champion, Y. & Hÿtch, M. J. HRTEM study of defects in twin boundaries of ultra-fine grained copper. *Philos. Mag.* **87**, 1465–1486 (2007).
30. Zhu, Y. T., Liao, X. Z. & Wu, X. L. Deformation twinning in nanocrystalline materials. *Prog. Mater. Sci.* **57**, 1–62 (2012).
31. Liu, L., Wang, J., Gong, S. K. & Mao, S. X. High resolution transmission electron microscope observation of zero-strain deformation twinning mechanisms in Ag. *Phys. Rev. Lett.* **106**, 175504 (2011).
32. Rice, J. R. Dislocation nucleation from a crack tip: an analysis based on the Peierls concept. *J. Mech. Phys. Solids* **40**, 239–271 (1992).

Acknowledgments

J.W. acknowledges the support provided by the US Department of Energy, Office of Science, Office of Basic Energy Sciences, and also acknowledges support provided by the Los Alamos National Laboratory Directed Research and Development (LDRD-ER20140450). S.X.M. would like to acknowledge NSF CMMI 0928517 through University of Pittsburgh. L.L. is supported by the Innovation Foundation of BUAA for PhD Graduates.

Author contributions

L.L. prepared the TEM sample and conducted the experiments. J.W. conducted the MD simulation. L.L., J.W. and S.X.M. prepared the manuscript. S.X.M. and S.K.G. made the plan. All the authors discussed the results and contributed to revising the paper.

Additional information

Supplementary information accompanies this paper at http://www.nature.com/scientificreports

Competing financial interests: The authors declare no competing financial interests.

How to cite this article: Liu, L., Wang, J., Gong, S.K. & Mao, S.X. Atomistic observation of a crack tip approaching coherent twin boundaries. *Sci. Rep.* **4**, 4397; DOI:10.1038/srep04397 (2014).